Z. Phys. C 59, 533–545 (1993)

ZEITSCHRIFT
FÜR PHYSIK C

A measurement of D meson production in Z^0 hadronic decays

DELPHI Collaboration

P. Abreu[20], W. Adam[7], T. Adye[37], E. Agasi[30], I. Ajinenko[43], R. Aleksan[39], G.D. Alekseev[14], A. Algeri[13], P. Allen[49], A. Almehed[23], S.J. Alvsvaag[4], U. Amaldi[7], A. Andreazza[27], P. Antilogus[24], W.-D. Apel[15], R.J. Apsimon[37], Y. Arnoud[39], B. Åsman[45], J.-E. Augustin[18], A. Augustinus[30], P. Baillon[7], P. Bambade[18], F. Barao[20], R. Barate[12], G. Barbiellini[47], D.Y. Bardin[14], G.J. Barker[34], A. Baroncelli[41], O. Barring[7], J.A. Barrio[25], W. Bartl[50], M.J. Bates[37], M. Battaglia[13], M. Baubillier[22], K.-H. Becks[52], C.J. Beeston[34], M. Begalli[36], P. Beilliere[6], Yu. Belokopyptov[43], P. Beltran[9], D. Benedic[8], A.C. Benvenuti[5], M. Berggren[18], D. Bertrand[2], F. Bianchi[46], M.S. Bilenky[14], P. Billoir[22], J. Bjarne[23], D. Bloch[8], S. Blyth[34], V. Bocci[38], P.N. Bogolubov[14], T. Bolognese[39], M. Bonesini[27], W. Bonivento[27], P.S.L. Booth[21], G. Borisov[43], H. Borner[7], C. Bosio[41], B. Bostjancic[44], S. Bosworth[34], O. Botner[48], B. Bouquet[18], C. Bourdarios[18], T.J.V. Bowcock[21], M. Bozzo[11], S. Braibant[2], P. Branchini[41], K.D. Brand[35], R.A. Brenner[7], H. Briand[22], C. Bricman[2], R.C.A. Brown[7], N. Brummer[30], J.-M. Brunet[6], L. Bugge[32], T. Buran[32], H. Burmeister[7], J.A.M.A. Buytaert[7], M. Caccia[7], M. Calvi[27], A.J. Camacho Rozas[42], R. Campion[21], T. Camporesi[7], V. Canale[38], F. Cao[2], F. Carena[7], L. Carroll[21], M.V. Castillo Gimenez[49], A. Cattai[7], F.R. Cavallo[5], L. Cerrito[38], V. Chabaud[7], A. Chan[1], M. Chapkin[43], Ph. Charpentier[7], L. Chaussard[18], J. Chauveau[22], P. Checchia[35], G.A. Chelkov[14], L. Chevalier[39], P. Chliapnikov[43], V. Chorowicz[22], J.T.M. Chrin[49], P. Collins[34], J.L. Contreras[25], R. Contri[11], E. Cortina[49], G. Cosme[18], F. Couchot[18], H.B. Crawley[1], D. Crennell[37], G. Crosetti[11], M. Crozon[6], J. Cuevas Maestro[33], S. Czellar[13], E. Dahl-Jensen[28], B. Dalmagne[18], M. Dam[32], G. Damgaard[28], G. Darbo[11], E. Daubie[2], A. Daum[15], P.D. Dauncey[34], M. Davenport[7], P. David[22], J. Davies[21], W. Da Silva[22], C. Defoix[6], P. Delpierre[6], N. Demaria[46], A. De Angelis[47], H. De Boeck[2], W. De Boer[15], C. De Clerq[2], M.D.M. De Fez Laso[49], N. De Groot[30], C. De La Vaissiere[22], B. De Lotto[47], A. De Min[27], H. Dijkstra[7], L. Di Ciaccio[38], J. Dolbeau[6], M. Donszelmann[7], K. Doroba[51], M. Dracos[7], J. Drees[52], M. Dris[31], Y. Dufour[7], F. Dupont[12], D. Edsall[1], L.-O. Eek[48], P.A.-M. Eerola[7], R. Ehret[15], T. Ekelof[48], G. Ekspong[45], A. Elliot Peisert[35], J.-P. Engel[8], N. Ershaidat[22], D. Fassouliotis[31], M. Feindt[7], A. Fenyuk[43], M. Fernandez Alonso[42], A. Ferrer[49], T.A. Filippas[31], A. Firestone[1], H. Foeth[7], E. Fokitis[31], F. Fontanelli[11], K.A.J. Forbes[21], J.-L. Fousset[26], S. Francon[24], B. Franek[37], P. Frenkiel[6], D.C. Fries[15], A.G. Frodesen[4], R. Fruhwirth[50], F. Fulda-Quenzer[18], K. Furnival[21], H. Furstenau[15], J. Fuster[7], D. Gamba[46], C. Garcia[49], J. Garcia[42], C. Gaspar[7], U. Gasparini[35], Ph. Gavillet[7], E.N. Gazis[31], J.-P. Gerber[8], P. Giacomelli[7], R. Gokieli[51], B. Golob[44], V.M. Golovatyuk[14], J.J. Gomez Y Cadenas[7], G. Gopal[37], M. Gorski[51], V. Gracco[11], A. Grant[7], F. Grard[2], E. Graziani[41], G. Grosdidier[18], E. Gross[7], P. Grosse-Wiesmann[7], B. Grossetete[22], J. Guy[37], U. Haedinger[15], F. Hahn[52], M. Hahn[15], S. Haider[30], Z. Hajduk[16], A. Hakansson[23], A. Hallgren[48], K. Hamacher[52], G. Hamel De Monchenault[39], W. Hao[30], F.J. Harris[34], V. Hedberg[23], T. Henkes[7], J.J. Hernandez[49], P. Herquet[2], H. Herr[7], T.L. Hessing[21], I. Hietanen[13], C.O. Higgins[21], E. Higon[49], H.J. Hilke[7], S.D. Hodgson[34], T. Hofmokl[51], R. Holmes[1], S.-O. Holmgren[45], D. Holthuizen[30], P.F. Honore[6], J.E. Hooper[28], M. Houlden[21], J. Hrubec[50], K. Huet[2], P.O. Hulth[45], K. Hultqvist[45], P. Ioannou[3], P.-S. Iversen[4], J.N. Jackson[21], P. Jalocha[16], G. Jarlskog[23], P. Jarry[39], B. Jean-Marie[18], E.K. Johansson[45], D. Johnson[21], M. Jonker[7], L. Jonsson[23], P. Juillot[8], G. Kalkanis[3], G. Kalmus[37], F. Kapusta[22], M. Karlsson[7], E. Karvelas[9], S. Katsanevas[3], E.C. Katsoufis[31], R. Keranen[7], J. Kesteman[2], B.A. Khomenko[14], N.N. Khovanski[14], B. King[21], N.J. Kjaer[7], H. Klein[7], A. Klovning[4], P. Kluit[30], A. Koch-Mehrin[52], J.H. Köhne[15], B. Koene[30], P. Kokkinias[9], M. Koratzinos[32], K. Korcyl[16], A.V. Korytov[14], V. Kostioukhine[43], C. Kourkoumelis[3], O. Kouznetsov[14], P.H. Kramer[52], J. Krolikowski[51], I. Kronkvist[23], U. Kruener-Marquis[52], W. Kucewicz[16], K. Kulka[48], K. Kurvinen[13], C. Lacasta[49], C. Lambropoulos[9], J.W. Lamsa[1], L. Lanceri[47], V. Lapin[43], J.-P. Laugier[39], R.Lauhakangas[13], G. Leder[50], F. Ledroit[12], R. Leitner[29], Y. Lemoigne[39], J. Lemonne[2], G. Lenzen[52], V. Lepeltier[18], T. Lesiak[16], J.M. Levy[8], E. Lieb[52], D. Liko[50], J. Lindgren[13], R. Lindner[52], A. Lipniacka[51], I. Lippi[35], B. Loerstad[23], M. Lokajicek[10], J.G. Loken[34], A. Lopez-Fernandez[7], M.A. Lopez Aguera[42], M. Los[30], D. Loukas[9], J.J. Lozano[49], P. Lutz[6], L. Lyons[34], G. Maehlum[32], J. Maillard[6], A. Maio[20], A. Maltezos[9], F. Mandl[50], J. Marco[42], M. Margoni[35], J.-C. Marin[7], A. Markou[9], T. Maron[52], S. Marti[49], L. Mathis[1], F. Matorras[42], C. Matteuzzi[27], G. Matthiae[38], M. Mazzucato[35], M. Mc Cubbin[21], R. Mc Kay[1], R. Mc Nulty[21], G. Meola[11], C. Meroni[27], W.T. Meyer[1], M. Michelotto[35], I. Mikulec[50], L. Mirabito[24], W.A. Mitaroff[50], G.V. Mitselmakher[14], U. Mjoernmark[23], T. Moa[45], R. Moeller[28], K. Moenig[7], M.R. Monge[11], P. Morettini[11], H. Mueller[15], W.J. Murray[37], G. Myatt[34], F.L. Navarria[5], P. Negri[27], R. Nicolaidou[3], B.S. Nielsen [28], B. Nijjhar[21], V. Nikolaenko[43], P.E.S. Nilsen[4], P. Niss[45], A. Nomerotski[35], V. Obraztsov[43], A.G. Olshevski[14], R. Orava[13], A. Ostankov[43], K. Osterberg[13], A. Ouraou[39], M. Paganoni[27], R. Pain[22], H. Palka[16], Th.D. Papadopoulou[31], L. Pape[7], F. Parodi[11], A. Passeri[41], M. Pegoraro[35], J. Pennanen[13], L. Peralta[20], H. Pernegger[50], M. Pernicka[50], A. Perrotta[5], C. Petridou[47], A. Petrolini[11], F. Pierre[39], M. Pimenta[20], O. Pingot[2], S. Plaszczynski[18], O. Podobrin[15], M.E. Pol[17], G. Polok[16], P. Poropat[47],

V. Pozdniakov[14], P. Privitera[15], A. Pullia[27], D. Radojicic[34], S. Ragazzi[27], H. Rahmani[31], P.N. Ratoff[19], A.L. Read[32], P. Rebecchi[7], N.G. Redaelli[27], M. Regler[50], D. Reid[7], P.B. Renton[34], L.K. Resvanis[3], F. Richard[18], M. Richardson[21], J. Ridky[10], G. Rinaudo[46], I. Roditi[17], A. Romero[46], I. Roncagliolo[11], P. Ronchese[35], C. Ronnqvist[13], E.I. Rosenberg[1], S. Rossi[7], E. Rosso[7], P. Roudeau[18], T. Rovelli[5], W. Ruckstuhl[30], V. Ruhlmann-Kleider[39], A. Ruiz[42], H. Saarikko[13], Y. Sacquin[39], G. Sajot[12], J. Salt[49], J. Sanchez[25], M. Sannino[11,40], S. Schael[7], H. Schneider[15], M.A.E. Schyns[52], G. Sciolla[46], F. Scuri[47], A.M. Segar[34], A. Seitz[15], R. Sekulin[37], M. Sessa[47], G. Sette[11], R. Seufert[15], R.C. Shellard[36], I. Siccama[30], P. Siegrist[39], S. Simonetti[11], F. Simonetto[35], A.N. Sisakian[14], G. Skjevling[32], G. Smadja[39,24], O. Smirnova[14], G.R. Smith[37], R. Sosnowski[51], D. Souza-Santos[36], T.S. Spassoff[12], E. Spiriti[41], S. Squarcia[11], H. Staeck[52], C. Stanescu[41], S. Stapnes[32], G. Stavropoulos[9], F. Stichelbaut[2], A. Stocchi[18], J. Strauss[50], J. Straver[7], R. Strub[8], B. Stugu[4], M. Szczekowski[7], M. Szeptycka[51], P. Szymanski[51], T. Tabarelli[27], O. Tchikilev[43], G.E. Theodosiou[9], A. Tilquin[26], J. Timmermans[30], V.G. Timofeev[14], L.G. Tkatchev[14], T. Todorov[8], D.Z. Toet[30], O. Toker[13], B. Tome[20], E. Torassa[46], L. Tortora[41], D. Treille[7], U. Trevisan[11], W. Trischuk[7], G. Tristram[6], C. Troncon[27], A. Tsirou[7], E.N. Tsyganov[14], M.-L. Turluer[39], T. Tuuva[13], I.A. Tyapkin[22], M. Tyndel[37], S. Tzamarias[21], S. Ueberschaer[52], O. Ullaland[7], V. Uvarov[43], G. Valenti[5], E. Vallazza[46], J.A. Valls Ferrer[49], C. Vander Velde[2], G.W. Van Apeldoorn[30], P. Van Dam[30], M. Van Der Heijden[30], W.K. Van Doninck[2], P. Vaz[7], G. Vegni[27], L. Ventura[35], W. Venus[37], F. Verbeure[2], M. Verlato[35], L.S. Vertogradov[14], D. Vilanova[39], P. Vincent[24], L. Vitale[13], E. Vlasov[43], A.S. Vodopyanov[14], M. Vollmer[52], M. Voutilainen[13], V. Vrba[41], H. Wahlen[52], C. Walck[45], F. Waldner[47], M. Wayne[1], A. Wehr[52], M. Weierstall[52], P. Weilhammer[7], J. Werner[52], A.M. Wetherell[7], J.H. Wickens[2], G.R. Wilkinson[34], W.S.C. Williams[34], M. Winter[8], M. Witek[16], G. Wormser[18], K. Woschnagg[48], N. Yamdagni[45], P. Yepes[7], A. Zaitsev[43], A. Zalewska[16], P. Zalewski[18], D. Zavrtanik[44], E. Zevgolatakos[9], G. Zhang[52], N.I. Zimin[14], M. Zito[39], R. Zuberi[34], R. Zukanovich Funchal[6], G. Zumerle[35], J. Zuniga[49]

[1] Ames Laboratory and Department of Physics, Iowa State University, Ames, IA 50011, USA
[2] Physics Department, Univ. Instelling Antwerpen, Universiteitsplein 1, B-2610 Wilrijk, Belgium, and IIHE, ULB-VUB, Pleinlaan 2, B-1050 Brussels, Belgium, and Faculté des Sciences, Univ. de l'Etat Mons, Av. Maistriau 19, B-7000 Mons, Belgium
[3] Physics Laboratory, University of Athens, Solonos Str. 104, GR-10680 Athens, Greece
[4] Department of Physics, University of Bergen, Allégaten 55, N-5007 Bergen, Norway
[5] Dipartimento di Fisica, Università di Bologna and INFN, Via Irnerio 46, I-40126 Bologna, Italy
[6] Collège de France, Lab. de Physique Corpusculaire, IN2P3-CNRS, F-75231 Paris Cedex 05, France
[7] CERN, CH-1211 Geneva 23, Switzerland
[8] Centre de Recherche Nucléaire, IN2P3, CNRS/ULP, BP20, F-67037 Strasbourg Cedex, France
[9] Institute of Nuclear Physics, N.C.S.R. Demokritos, P.O. Box 60228, GR-15310 Athens, Greece
[10] FZU, Inst. of Physics of the C.A.S. High Energy Physics Division, Na Slovance 2, CS-180 40, Praha 8, Czech. Republic
[11] Dipartimento di Fisica, Università di Genova and INFN, Via Dodecaneso 33, I-16146 Genova, Italy
[12] Institut des Sciences Nucléaires, IN2P3-CNRS, Université de Grenoble 1, F-38026 Grenoble, France
[13] Research Institute for High Energy Physics, SEFT, Siltavuorenpenger 20C, SF-00170 Helsinki, Finland
[14] Joint Institute for Nuclear Research, Dubna, Head Post Office, P.O. Box 79, 101 000 Moscow, Russian Federation
[15] Institut für Experimentelle Kernphysik, Universität Karlsruhe, Postfach 6980, D-76128 Karlsruhe 1, Germany
[16] High Energy Physics Laboratory, Institute of Nuclear Physics, Ul. Kawiory 26a, PL-30055 Krakow 30, Poland
[17] Centro Brasileiro de Pesquisas Fisicas, rua Xavier Sigaud 150, RJ-22290 Rio de Janeiro, Brazil
[18] Université de Paris-Sud, Lab. de l'Accélérateur Linéaire, IN2P3-CNRS, Bat 200, F-91405 Orsay, France
[19] School of Physics and Materials, University of Lancaster, Lancaster LA1 4YB, UK
[20] LIP, IST, FCUL, Av. Elias Garcia, 14, 1°, P-1000 Lisboa Codex, Portugal
[21] Department of Physics, University of Liverpool, P.O. Box 147, Liverpool L69 3BX, UK
[22] LPNHE, IN2P3-CNRS, Universités Paris VI et VII, Tour 33 (RdC), 4 place Jussieu, F-75252 Paris Cedex 05, France
[23] Department of Physics, University of Lund, Sölvegatan 14, S-22363 Lund, Sweden
[24] Université Claude Bernard de Lyon, IPNL, IN2P3-CNRS, F-69622 Villeurbanne Cedex, France
[25] Universidad Complutense, Avda. Complutense s/n, E-28040 Madrid, Spain
[26] Univ. d'Aix, Marseille II, CPP, IN2P3-CNRS, F-13288 Marseille Cedex 09, France
[27] Dipartimento di Fisica, Università di Milano and INFN, Via Celoria 16, I-20133 Milan, Italy
[28] Niels Bohr Institute, Blegdamsvej 17, DK-2100 Copenhagen O, Denmark
[29] NC, Nuclear Centre of MFF, Charles University, Areal MFF, V Holesovickach 2, CS-180 00, Praha 8, Czech. Republic
[30] NIKHEF-H, Postbus 41882, 1009 DB Amsterdam, The Netherlands
[31] National Technical University, Physics Department, Zografou Campus, GR-15773 Athens, Greece
[32] Physics Department, University of Oslo, Blindern, N-1000 Oslo 3, Norway
[33] Dpto. Fisica, Univ. Oviedo, C/P. Jimenez Casas, S/N, E-33006 Oviedo, Spain
[34] Department of Physics, University of Oxford, Keble Road, Oxford OX1 3RH, UK
[35] Dipartimento di Fisica, Università di Padova and INFN, Via Marzolo 8, I-35131 Padua, Italy
[36] Depto. de Fisica, Pontificia Univ. Católica, C.P. 38071, RJ-22453 Rio de Janeiro, Brazil
[37] Rutherford Appleton Laboratory, Chilton, GB-Didcot OX11 OQX, UK
[38] Dipartimento di Fisica, Università di Roma II and INFN, Tor Vergata, I-00173 Rome, Italy
[39] Centre d'Etude de Saclay, DSM/DAPNIA, F-91191 Gif-sur-Yvette Cedex, France
[40] Dipartimento di Fisica, Università di Salerno, I-84100 Salerno, Italy
[41] Istituto Superiore di Sanità, Ist. Naz. di Fisica Nucl. (INFN), Viale Regina Elena 299, I-00161 Rome, Italy
[42] C.E.A.F.M., C.S.I.C., Univ. Cantabria, Avda. los Castros, S/N, E-39006 Santander, Spain
[43] Inst. for High Energy Physics, Serpukov P.O. Box 35, Protvino, (Moscow Region), Russian Federation
[44] J. Stefan Institute and Department of Physics, University of Ljubljana, Jamova 39, SI-61000 Ljubljana, Slovenia
[45] Institute of Physics, University of Stockholm, Vanadisvägen 9, S-113 46 Stockholm, Sweden

[46] Dipartimento di Fisica Sperimentale, Università di Torino and INFN, Via P. Giuria 1, I-10125 Turin, Italy
[47] Dipartimento di Fisica, Università di Trieste and INFN, Via A. Valerio 2, I-34127 Trieste, Italy, and Istituto di Fisica, Università di Udine, I-33100 Udine, Italy
[48] Department of Radiation Sciences, University of Uppsala, P.O. Box 535, S-751 21 Uppsala, Sweden
[49] IFIC, Valencia-CSIC, and D.F.A.M.N., U. de Valencia, Avda. Dr. Moliner 50, E-46100 Burjassot (Valencia), Spain
[50] Institut für Hochenergiephysik, Österr. Akad. d. Wissensch., Nikolsdorfergasse 18, A-1050 Vienna, Austria
[51] Inst. Nuclear Studies and University of Warsaw, Ul. Hoza 69, PL-00681 Warsaw, Poland
[52] Fachbereich Physik, University of Wuppertal, Postfach 100 127, D-42097 Wuppertal 1, Germany

Received 12 May 1993

Abstract. A study of the fragmentation properties of charm and bottom quarks into D mesons is presented. From 263 700 Z^0 hadronic decays collected in 1991 with the DELPHI detector at the LEP collider, D^0, D^+ and D^{*+} are reconstructed in the modes $K^-\pi^+$, $K^-\pi^+\pi^+$ and $D^0\pi^+$ followed by $D^0\to K^-\pi^+$, respectively. The fractional decay widths $\Gamma(Z^0\to D/\bar{D}X)/\Gamma_h$ are determined, and first results are presented for the production of D mesons from $c\bar{c}$ and $b\bar{b}$ events separately. The average energy fraction of $D^{*\pm}$ in charm quark fragmentation is found to be $\langle X_E(D^*)\rangle_c = 0.487 \pm 0.015$ (stat) ± 0.005 (sys.). Assuming that the fraction of D_s and charm-baryons produced at LEP is similar to that around 10 GeV, the Z^0 partial width into charm quark pairs is determined to be $\Gamma_c/\Gamma_h = 0.187 \pm 0.031$ (stat) ± 0.023 (sys). The probability for a b quark to fragment into $\bar{B}_s$ or b-baryons is inferred to be 0.268 ± 0.094 (stat) ± 0.100 (sys) from the measured probability that it fragments into a $\bar{B}^0$ or B^-.

1 Introduction

D mesons are known to be abundantly produced in the fragmentation and decay of c and b quarks. The charm quark fragments directly to the D, whereas the bottom quark fragments first into a B which subsequently decays to a D. This difference in the hadronization leads to energetic D mesons from primary charm quarks and a softer spectrum from bottom quarks.

An analysis of the production of D^0, D^+ and D^{*+} mesons* is presented using Z^0 hadronic decays collected in 1991 at LEP with the DELPHI detector. Charmed mesons are reconstructed in the following channels:

- $D^{*+}\to D^0\pi^+$ followed by $D^0\to K^-\pi^+$
- $D^0\to K^-\pi^+$
- $D^+\to K^-\pi^+\pi^+$.

In the last two channels, the kaon is tagged by the ionization measurements made in the time projection Chamber. The silicon strip vertex detector helps separate primary and secondary vertices and improves the momentum resolution of charged particles.

After a brief description of the detector, the selection of Z^0 hadronic events and the Monte Carlo simulation are presented in Sect. 2. The methods for vertex reconstruction and the selections made for the various D mesons are detailed in Sect. 3. In Sect. 4 the results of the fits to the D meson energy spectra are given and compared in Sect. 5 to 7 with previous analyses performed around the Υ_{4S}.

* Throughout the paper charge-conjugate states are implicitly included

2 The detector, event selection and simulation

A description of the DELPHI apparatus can be found in [1]. Only tracking detectors for charged particles were relevant for the present analysis: the vertex-detector (VD), the inner detector (ID), the time projection chamber (TPC), the outer detector (OD) and the forward chambers A and B (FCA, FCB). The coordinate system is defined by the polar angle θ to the electron beam direction, z, the azimuthal angle ϕ and the radius R.

In 1991 the vertex detector consisted of three layers of silicon, at radii 6.3 cm, 9.0 cm and 11.0 cm. The layers allowed $R\phi$ coordinates to be measured over a length in z of 24 cm, and defined an acceptance for polar angles of 27–153°, 37–143° and 42–138° for hits in the first, second and third layers, respectively. The residual of a hit in the inner layer relative to a charged particle with hits associated in the outer layers was measured to have an average resolution of 9.0 μm [2].

The TPC, the principal tracking device of DELPHI is a cylinder of 30 cm inner radius, 122 cm outer radius and has a length of 2.7 m divided into two halves separated by the high voltage plane. Each half is divided into 6 sectors, each with 192 sense wires used for the particle identification. The dE/dx energy loss of a charged particle is measured by these wires as the 80% truncated mean of the amplitudes of the wire signals. According to the study presented in Sect. 3.1 for particles from D^0 decays, the dE/dx resolution has been measured to be 7.5%. However 25% of charged particles with momentum above 1 GeV/c have no dE/dx information because they are too close to another track or have too few wire hits (a minimum of 30 wires was required).

By using the combined information from OD + TPC + ID + VD tracking detectors a resolution of 3.5% on $\sigma(p)/p$ was obtained for 45 GeV/c muons. Charged particles were retained if they satisfied the following selection criteria:

- momentum between 0.4 GeV/c and 50 GeV/c;
- relative error on momentum measurement less than 100%;

- more than 30 cm track length in the TPC;
- distance to the nominal interaction point along the beam direction below 10 cm;
- projection of impact parameter relative to the interaction point in the plane transverse to the beam direction less than 4 cm.

These selections allow a reliable measurement of the multiplicity and momentum of the charged particles. Hadronic events were then accepted by requiring:

- five or more charged particles;
- total energy of the charged particles greater than 12% of the centre-of-mass energy, assuming all charged particles to be pions.

A total of 250 500 hadronic events was selected from the 1991 data sample at centre-of-mass energies between 88.2 GeV and 94.2 GeV. This corresponds to 263 700 Z^0 hadronic decays when corrected for the selection efficiency which was determined by Monte Carlo simulation as described below.

Simulated hadronic events have been generated using the Lund parton shower Monte Carlo program [3]. The fragmentation parameters of the simulation* were tuned from various event-shape distributions observed in DELPHI hadronic final states [4]. The fragmentation of c and b quarks was described in the Lund string fragmentation model by the Peterson fragmentation function [5]:

$$D_q(z) \propto \frac{1}{z \cdot [1-(1/z)-\varepsilon_q/(1-z)]^2}, \quad (1)$$

where $z=(E+p_l)_{\text{hadron}}/(E+p)_{q=c,b}$, p_l being the longitudinal momentum relative to the quark axis. For b quark fragmentation, the Peterson coefficient $\varepsilon_b = 0.008^{+0.005}_{-0.004}$ was used [6]. The analysis presented in Sect. 4 describes the measurement of the Peterson coefficient, ε_c, for c quark fragmentation.

Only D or D^* mesons were produced in the charm quark fragmentation, or in B meson decay, with a rate $D^*/D=3$. No D^{**} production was considered, apart from a 20% contribution in B meson semi-leptonic decays. The D^{**} contribution in the charm quark fragmentation and in B meson decays will be discussed in Sect. 5.

The events were followed through the detailed detector simulation DELSIM [7] which included simulation of secondary interactions and digitization of all electronic signals. The simulated data were then processed through the same analysis chain as the real data. The Z^0 hadronic decay selection efficiency was thus estimated to be $95.0 \pm 0.4\%$. A total of 700 000 Z^0 hadronic events was simulated for background studies, and 10 000 events were generated in each D^0, D^+ and D^{*+} decay channel in order to estimate the D meson acceptance and reconstruction efficiency.

* The relevant parameters were: effective $\Lambda_{\text{QCD}}=255$ eV, invariant mass cut-off $Q_0=1.3$ GeV/c^2, transverse momentum spread $\sigma(p_T)=0.395$ GeV/c for primary hadrons; the fragmentation of light quark flavours was described by the "symmetric Lund fragmentation function" with coefficients $a=0.18$ and $b=0.34$ GeV^{-2}

3 Charmed meson reconstruction

The analysis of charmed mesons was based on the separation between primary and secondary vertices and on kaon assignment using the dE/dx information. A more detailed description of the D meson reconstruction is presented in Sect. 3.1 to 3.3. Only the part common to each analysis is summarized here.

The mean transverse position of the beam, known for each fill, was added as a constraint into a primary vertex fit. The measured r.m.s. widths of the beam spot in the horizontal and vertical directions were 150 μm and 20 μm, respectively. Charged particles were assigned to the primary interaction vertex by a two-stage impact parameter cut: first a loose cut (0.75 cm) with respect to the beam spot, then a tighter one (0.30 cm) with respect to the vertex from the first iteration.

Depending on whether the D^0 or D^+ decay final state was considered, a $K^-\pi^+$ or $K^-\pi^+\pi^+$ combination was selected to compute a secondary vertex in space. The D^0 or D^+ momentum was calculated by the sum of the momenta of the decay products from this secondary vertex. Charged particles were considered if they had momentum above 1 GeV/c, and the energy fraction, $X_E(D)=E(D)/E_{\text{beam}}$, of the D meson was required to exceed 0.15.

As the fitted vertex positions was most precise in the $R\phi$ plane, the distance between the primary and secondary vertices was calculated in this transverse plane. This distance was given the same sign as the scalar product of the D momentum with the vector joining the primary to the secondary vertices. Its length in space was then computed using the direction of the D meson. This signed apparent decay length in space, ΔL, was required to lie between -0.5 cm and 2 cm in order to eliminate poorly reconstructed vertices.

Using the vertex detector, decay lengths can be measured with a resolution of about 300 μm in the transverse plane, or about 350 μm in space. This resolution is much smaller than the apparent decay length of charmed D mesons produced in $c\bar{c}$ events or in B meson decays, which are typically between 1.5 mm and 3 mm at LEP energies. The combinatorial background can be reduced by imposing a cut on $\Delta L/\sigma$, the signed apparent decay length divided by its measured error. An enriched sample of $b\bar{b}$ events was obtained as follows: the apparent proper time t of a reconstructed D meson is defined as $t=\Delta L \cdot M(D)/p(D)$ where $M(D)$ and $p(D)$ are the mass and momentum of the D meson. For a D meson from charm quark fragmentation, t is the D proper decay time and is on average 0.42 ps for D^0 and 1.07 ps for D^+ [8]. For a D^0 or D^+ from B decay, ΔL is greater than the D decay length whereas the D momentum is lower on average than for $c\bar{c}$ events. This results in an apparent proper time which is longer than the B proper time, assumed to be 1.3 ps on average in the following [9]. Selecting from the simulation decays with an apparent proper time greater than 1 ps would retain 9% of D^0 mesons from $c\bar{c}$ events and 60% of D^0 from $b\bar{b}$ events; whereas a selection of greater than 1.5 ps would retain 25% of D^+ mesons from $c\bar{c}$ events and 60% of D^+ from $b\bar{b}$ events.

In the following, whenever the normalised decay length $\Delta L/\sigma$ or the apparent proper time t is considered, the vertex detector is required to have been used in the track fit for at least two charged particles from the D^0 or D^+ decay candidates.

No particle identification was applied in the $D^{*+} \to (K^- \pi^+)\pi^+$ decay mode, but this channel was used to check the $\mathrm{d}E/\mathrm{d}x$ information as shown in Sect. 3.1 and Fig. 3 below. For the D^0 or D^+ analysis, the measured $\mathrm{d}E/\mathrm{d}x$ of the kaon candidate was required to be at least one standard deviation below the theoretical energy loss of a pion.

The number of reconstructed D mesons was obtained by fitting the invariant mass (or the mass difference in the case of D^{*+}) distributions in different X_E intervals.

3.1 $D^{*+} \to (K^- \pi^+)\pi^+$

The selection criteria for the decay $D^{*+} \to D^0 \pi^+$ followed by $D^0 \to K^- \pi^+$ relied mainly on the small mass difference between D^{*+} and D^0 mesons, and on the peculiar kinematics of the pion from the D^{*+} decay, hereafter called the bachelor pion.

To reduce the combinatorial background, the angle θ^* between the D^0 flight direction and the kaon direction in the D^0 rest frame was required to satisfy the condition $\cos\theta^* > -0.6, -0.8, -0.9$ for $X_E(D^{*+})$ in the range 0.15–0.25, 0.25–0.5, 0.5–1, respectively. For genuine D^0 candidates an isotropic distribution in $\cos\theta^*$ is expected whereas the background is strongly peaked in the backward direction.

The mass difference $\Delta M = M(\text{“}D^0\text{”}\pi^+) - M(\text{“}D^0\text{”})$ was computed by adding in turn all possible bachelor pions to the “D^0” combination, where “D^0” refers here to candidate $K^-\pi^+$ pairs without their mass being constrained to the D^0 mass. In order to reject poorly measured tracks, only charged particles with an impact parameter lower than 0.3 cm with respect to the primary vertex were retained as bachelor pion candidates. The four-momentum of these candidates was calculated after the primary vertex fit. These requirements improve the ΔM resolution and the signal-to-noise ratio without loss of genuine D^{*+} from B decays. The bachelor pion momentum had to be between 0.3 GeV/c and 4.5 GeV/c, corresponding to $X_E(D^{*+})$ between 0.15 and 1.

The invariant mass $(K^-\pi^+)$ and the mass difference ΔM are shown in Fig. 1a and b, respectively. The mass difference distribution is given for a $(K^-\pi^+)$ mass interval between 1.79 GeV/c^2 and 1.94 GeV/c^2. The $(K^-\pi^+)$ mass is given for ΔM between 0.1435 GeV/c^2 and 0.1475 GeV/c^2. The hatched histograms (scaled up by a factor 2) are the same distributions for X_E above 0.55 where the combinatorial background is significantly reduced. The $(K^-\pi^+)$ mass distribution was fitted by using the following contributions: an exponential function for the combinatorial background, a Gaussian function for the $D^0 \to K^-\pi^+$ events, and a parameterization from the Monte Carlo simulation of the $D^0 \to K^-\pi^+(\pi^0)$ contribution which appears as a shoulder below 1.7 GeV/c^2. The measured $(K^-\pi^+)$ mass is 1.859 ± 0.003 GeV/c^2, about two standard deviations

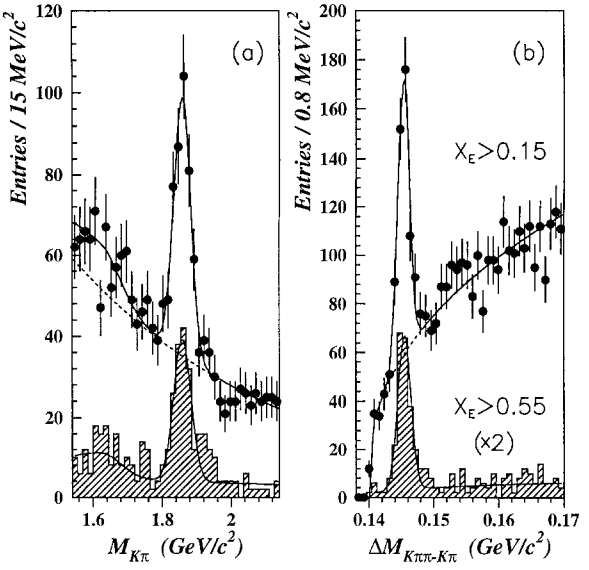

Fig. 1a, b. The invariant mass $M(K^-\pi^+)$ **a** and $\Delta M = M(K^-\pi^+\pi^+) - M(K^-\pi^+)$ **b** distributions for events with $X_E = E(K^-\pi^+\pi^+)/E_{\text{beam}}$ above 0.15. The $(K^-\pi^+)$ mass distribution is presented for ΔM in the range 0.1435–0.1475 GeV/c^2. The mass difference distribution is presented for a $(K^-\pi^+)$ mass between 1.79 GeV/c^2 and 1.94 GeV/c^2. The solid line curves are fits as described in the text. The dashed lines show the background contribution to the fits. The hatched histograms (scaled up by a factor 2) are the same experimental distributions for X_E above 0.55

lower than the expected D^0 mass [8], and the experimental resolution is 24 ± 3 MeV/c^2. This mass shift, which is also observed for the direct D^0 analysis (see Sect. 3.2) and with less significance for the D^+ (see Sect. 3.3), could be due to residual alignment errors of the detectors used in the tracking.

The signal in the mass difference distribution was described by a Gaussian function, and the background by the function $\alpha(\Delta M - m_\pi)^\beta$. In order to have a better description of the background, especially at low X_E, the exponent β was determined using two different background estimates:

- In the first case the upper side band (2.1 GeV/c^2 to 2.5 GeV/c^2) of the $(K^-\pi^+)$ mass distribution was used with the same selection criteria as for the D^{*+}, yielding a value for β of 0.44 ± 0.02.
- In the second case only particles with charge opposite to the bachelor pion were required in a $(K^-\pi^-)$ mass combination: the selections in $\cos\theta^*$ and in distance between vertices were removed, and the $(K^-\pi^-)$ mass combination was taken between 1.80 GeV/c^2 and 1.92 GeV/c^2. The obtained value for β was 0.43 ± 0.02.

The fitted parameters were thus the normalisation, the central value and the width of the Gaussian function, and the normalisation α of the background. The curve presented in Fig. 1b is the result of a fit obtained by averaging the high mass and the same sign background shapes. Within statistical error both choices of the exponent β lead to compatible numbers of D^{*+}: 361 ± 25 and 355 ± 25, counted with the high $(K^-\pi^+)$ mass and with the $(K^-\pi^-)$ mass backgrounds, respectively, for

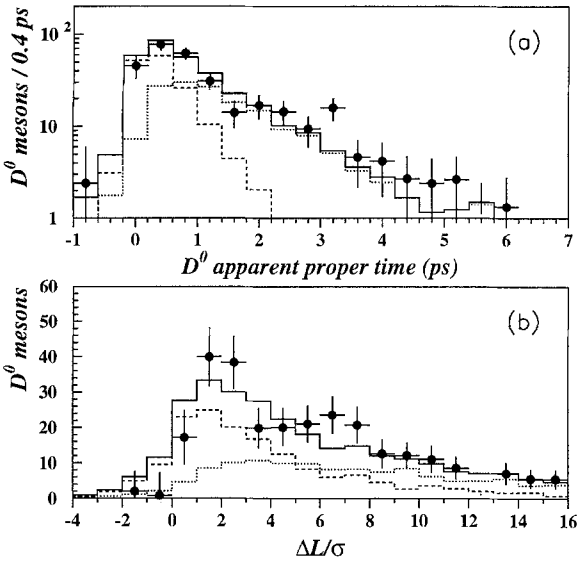

Fig. 2a, b. Apparent proper time distribution $t = \Delta L \cdot M(D^0)/p(D^0)$ **a** and normalised decay length $\Delta L/\sigma$ **b** for D^0 mesons from D^{*+} with $X_E(D^{*+})$ above 0.15, where both tracks $(K^-\pi^+)$ have hits in the vertex detector. The measured distribution after background subtraction is shown with data points. The simulated D^0 from $c\bar{c}$ events (dashed histogram), simulated D^0 from $b\bar{b}$ events (dotted histogram), and sum of the $c\bar{c}$ and $b\bar{b}$ contributions (solid histogram) assume $\tau(B) = 1.3$ ps and $P_{b\to D^{*+}}/P_{c\to D^{*+}} = 0.87$

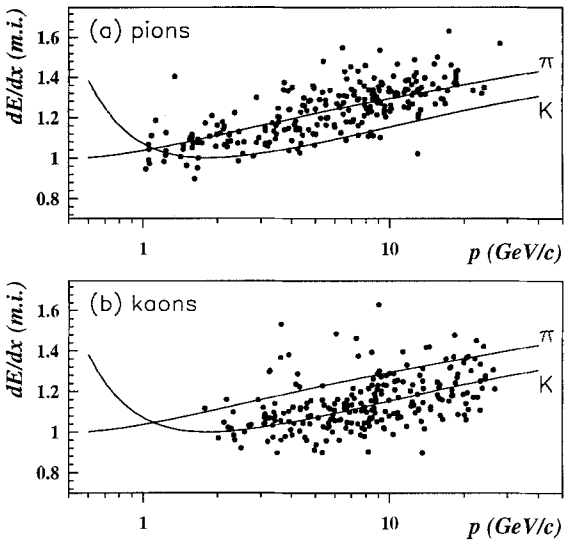

Fig. 3a, b. The measured dE/dx as a function of the momentum for **a** pion and **b** kaon candidates from reconstructed D^0 in $D^{*+} \to (K^-\pi^+)\pi^+$ decays. The dE/dx is expressed in units of minimum ionization. The curves are the expected ionization losses for pions and kaons

$X_E(D^{*+})$ above 0.15. The fitted value of ΔM is 0.1454 ± 0.0001 GeV/c^2 in good agreement with the $(D^{*+} - D^0)$ mass difference [8] and the resolution is 0.8 ± 0.1 MeV/c^2.

Figure 2a displays the experimental apparent proper time distribution for D^0 from D^{*+} with $X_E(D^{*+})$ above 0.15 and with the two tracks of the D^0 having hits in the vertex detector. The estimated background, as defined previously, has been subtracted. This distribution (data points) exhibits a tail at large positive proper time which is not described by the distribution of D^0 in simulated $c\bar{c}$ events (dashed histogram). This tail is close to the D^0 apparent proper time distribution from simulated B decays (dotted histogram, with a B lifetime of 1.3 ps). Figure 2b displays the normalised decay length $\Delta L/\sigma$ for the same D^0 candidates. The sum of $c\bar{c}$ and $b\bar{b}$ contributions (solid histograms) describes the experimental distributions well. Here the relative probabilities for b and c quarks to fragment into a D^{*+} meson are taken as $P_{b\to D^{*+}}/P_{c\to D^{*+}} = 0.87$, as quoted in Table 4 below. Selecting D^{*+} with a D^0 apparent proper time greater than 1 ps, as discussed previously, retains 125 ± 15 D^{*+} originating mainly from B meson decays.

The measured dE/dx distributions for pion and kaon candidates from D^0 mesons in these D^{*+} decays are presented in Fig. 3 as a function of the particle momentum. The observed ionization loss is in good agreement with the expectation. The mean dE/dx for a kaon with momentum above 3 GeV/c is about 1.6 standard deviations below the mean dE/dx for a pion.

3.2 $D^0 \to K^-\pi^+$

The selection criteria for $D^0 \to K^-\pi^+$ decays were similar to those already presented for the D^0 from D^{*+} decay, but the higher combinatorial background required in addition the following constraints:

- Each particle was required to have associated hits in the vertex detector.
- At least one particle had to be measured in the outer detector. The requirement improved the invariant mass resolution and the signal-to-noise ratio.
- The dE/dx information from the TPC was used to select the kaon candidate, as defined above. This reduced the "K" π combinatorial background by a factor 3.4 and kept about 70% of the genuine $D^0 \to K^-\pi^+$, when the dE/dx information was available.
- The χ^2 probability of the fit of the K^- and π^+ candidates to a secondary vertex in space had to be larger than 1%.

Two event samples were then selected:

1. A first sample where the normalised decay length $\Delta L/\sigma$ was required to be above 1. In the simulation, 73% of D^0 from $c\bar{c}$ events and 94% of D^0 from $b\bar{b}$ events were retained with this selection.
2. A $b\bar{b}$ enriched sample, obtained by requiring that the D^0 apparent proper time was greater than 1 ps. This procedure led to the rejection of 91% of D^0 from $c\bar{c}$ events.

Due to the different production rates and selection criteria, 30% of the D^0 samples were estimated to be also included in the previously defined D^{*+} sample.

The $(K^-\pi^+)$ mass distribution with $\Delta L/\sigma$ above 1 is presented in Fig. 4. A fit was performed where the combinatorial background was described by an exponential

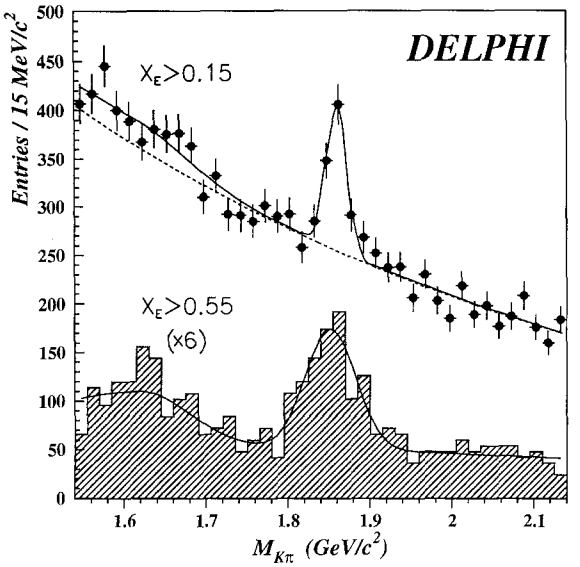

Fig. 4. $K^-\pi^+$ invariant mass distribution for X_E above 0.15 and normalised decay length $\Delta L/\sigma$ larger than 1. The kaon hypothesis is assigned from the dE/dx information. The solid line curves are fits as described in the text. The dashed line shows the background contribution to the fit. The hatched histogram (scaled up by a factor 6) is the same experimental distribution for X_E above 0.55

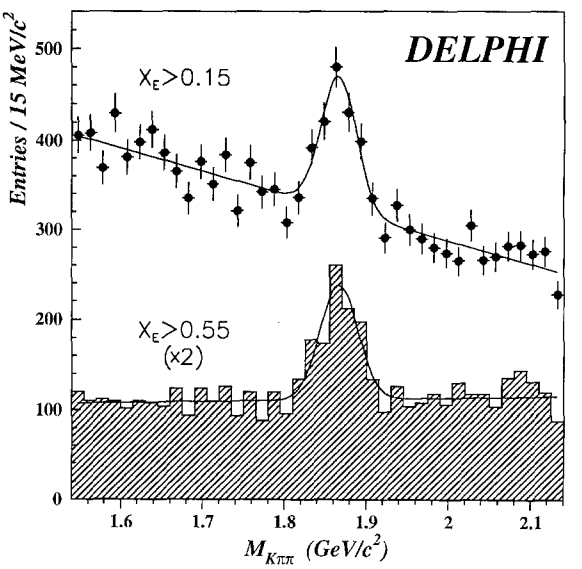

Fig. 5. $K^-\pi^+\pi^+$ invariant mass distribution for X_E above 0.15 and normalised decay length $\Delta L/\sigma > 3$. The kaon hypothesis is assigned from the dE/dx information for X_E below 0.55. The hatched histogram (scaled up by a factor 2) is the same experimental distribution for $X_E > 0.55$. The solid line curves are fits as described in the text

function, the $D^0 \to K^-\pi^+$ events were assigned a Gaussian shape, and another Gaussian function of r.m.s. width 170 MeV/c^2 described 15% of incorrectly assigned $K^+\pi^-$ pairs where the "kaon" candidate also fulfilled the dE/dx constraint. The $D^0 \to K^-\pi^+(\pi^0)$ contribution, where the π^0 was not observed, was parameterized according to the simulation by fixing the ratio $(D^0 \to K^-\pi^+\pi^0)/(D^0 \to K^-\pi^+)$ to 1.8, the relative branching fraction and acceptance of the $K^-\pi^+\pi^0$ decay channel. The measured D^0 mass is 1.860 ± 0.002 GeV/c^2, the $(K^-\pi^+)$ mass resolution is 12 ± 2 MeV/c^2 and 369 ± 40 D^0 are reconstructed. The hatched histogram (scaled up by a factor 6) corresponds to $K^-\pi^+$ pairs with X_E above 0.55: the $(K^-\pi^+)$ mass resolution is about 30 MeV/c^2 and 90 ± 14 D^0 are fitted with a better signal-to-noise ratio. Requiring an apparent proper time greater than 1 ps retains 159 ± 25 D^0 mesons with X_E above 0.15.

3.3 $D^+ \to K^-\pi^+\pi^+$

Compared to the D^0, the $D^+ \to K^-\pi^+\pi^+$ decay suffers from a higher combinatorial background, but benefits from the longer D^+ lifetime and from the unique kaon assignment in the three-particle combination. Slightly different selections were thus applied for this decay channel:

- At least two particles were required to have associated hits in the vertex detector.
- The momenta of the kaon and pion candidates had to exceed 2 GeV/c and 1 GeV/c, respectively.
- The impact parameter of each track with respect to the secondary vertex had to be lower than 100 μm.
- For X_E below 0.55, the kaon hypothesis was assigned using the dE/dx information. This requirement was not necessary above 0.55 due to the lower background.

Two event samples were then defined:

1. A first sample where the normalised decay length $\Delta L/\sigma$ was required to be above 3. This cut retains 69% of D^+ from $c\bar{c}$ events and 90% of D^+ from $b\bar{b}$ events.
2. A $b\bar{b}$ enriched sample, obtained by requiring that the D^+ apparent proper time was greater than 1.5 ps. This cut rejects 75% of D^+ from $c\bar{c}$ events. As the D^+ lifetime is close to the B lifetime, the $b\bar{b}$ purity of this sample was weaker than in the D^0 analysis.

The invariant mass distribution $(K^-\pi^+\pi^+)$ for the first sample is shown in Fig. 5. The D^+ signal, 539 ± 52 events, was fitted with a linear background and a Gaussian shape for the D^+ peak. Those $K^-\pi^+\pi^+$ candidates compatible with a $D^{*+} \to (K^-\pi^+)\pi^+$ decay were removed. The fitted D^+ mass is 1.867 ± 0.002 GeV/c^2, compatible with the expected value [8], and the resolution is 20 ± 2 MeV/c^2. The hatched histogram (scaled up by a factor 2) corresponds to $(K^-\pi^+\pi^+)$ events with X_E above 0.55, where the dE/dx information is not used: the $(K^-\pi^+\pi^+)$ mass resolution is about 23 MeV/c^2 and 247 ± 28 D^+ are fitted with a lower background. Requiring an apparent proper time greater than 1.5 ps retains 205 ± 28 D^+ mesons with X_E above 0.15.

4 Heavy quark fragmentation and D meson rates

The invariant mass spectra were fitted as described previously in eight X_E intervals ranging from 0.15 to 1. The

Table 1. $D^{*+}\to(K^-\pi^+)\pi^+$ data, showing the number $N(D^{*+})$ of fitted D mesons and their efficiencies (which include the geometrical acceptance and the reconstruction and selection efficiencies)

X_E	Full sample		Apparent proper time >1 ps		
	$N(D^{*+})\pm$(stat)	efficiency	$N(D^{*+})\pm$(stat)	eff. $c\bar{c}$	eff. $b\bar{b}$
0.15–0.25	41.1 ± 11.3	0.31	26.5 ± 8.6	0.02	0.17
0.25–0.35	101.4 ± 13.8	0.34	52.1 ± 8.8	0.03	0.18
0.35–0.45	58.4 ± 10.5	0.35	22.0 ± 5.7	0.03	0.17
0.45–0.55	52.9 ± 8.1	0.36	12.4 ± 4.0	0.03	0.16
0.55–0.65	53.2 ± 8.4	0.36	9.0 ± 3.3	0.03	0.15
0.65–0.75	36.0 ± 8.0	0.36	2.7 ± 1.8	0.03	0.14
0.75–0.85	13.5 ± 3.7	0.39	-	0.03	0.14
0.85–1.00	2.0 ± 2.0	0.39	-	0.03	0.12

Table 2. $D^0\to K^-\pi^+$ data

X_E	$\Delta L/\sigma>1$			Apparent proper time >1 ps		
	$N(D^0)\pm$(stat)	eff. $c\bar{c}$	eff. $b\bar{b}$	$N(D^0)\pm$(stat)	eff. $c\bar{c}$	eff. $b\bar{b}$
0.15–0.25	79.5 ± 24.7	0.10	0.13	42.5 ± 13.5	0.01	0.09
0.25–0.35	73.3 ± 19.6	0.09	0.11	35.5 ± 14.3	0.01	0.07
0.35–0.45	72.9 ± 17.7	0.09	0.11	48.4 ± 13.1	0.01	0.07
0.45–0.55	53.4 ± 10.8	0.09	0.11	15.9 ± 5.6	0.01	0.06
0.55–0.65	57.6 ± 10.4	0.10	0.13	6.9 ± 3.6	0.01	0.06
0.65–0.75	25.0 ± 7.5	0.11	0.13	7.9 ± 2.7	0.01	0.05
0.75–0.85	7.7 ± 5.3	0.11	0.13	1.4 ± 1.4	0.01	0.04
0.85–1.00	-	0.11	0.13	-	0.01	0.04

Table 3. $D^+\to K^-\pi^+\pi^+$ data

X_E	$\Delta L/\sigma>3$			Apparent proper time >1.5 ps		
	$N(D^+)\pm$(stat)	eff. $c\bar{c}$	eff. $b\bar{b}$	$N(D^+)\pm$(stat)	eff. $c\bar{c}$	eff. $b\bar{b}$
0.15–0.25	47.8 ± 20.0	0.06	0.08	38.7 ± 14.5	0.02	0.05
0.25–0.35	92.3 ± 26.3	0.08	0.10	34.5 ± 12.6	0.02	0.06
0.35–0.45	105.0 ± 24.6	0.09	0.12	51.6 ± 15.0	0.03	0.06
0.45–0.55	46.9 ± 14.1	0.10	0.12	18.9 ± 6.9	0.03	0.06
0.55–0.65	133.3 ± 21.9	0.26	0.32	35.6 ± 9.9	0.08	0.15
0.65–0.75	68.7 ± 14.1	0.26	0.32	21.5 ± 6.6	0.08	0.13
0.75–0.85	37.9 ± 8.2	0.26	0.32	4.0 ± 2.7	0.08	0.11
0.85–1.00	7.0 ± 4.2	0.26	0.32	1.0 ± 1.0	0.08	0.09

number of D mesons and their efficiencies are presented in Tables 1, 2 and 3 for D^{*+}, D^0 and D^+, respectively. The quoted efficiencies include the geometrical acceptance, the reconstruction efficiency and the $\mathrm{d}E/\mathrm{d}x$ constraint which do not depend on the original quark flavour of the event, and the selections on the normalised decay length or on the apparent proper time which are different if the D meson is produced in a $c\bar{c}$ or a $b\bar{b}$ event. In the following when combining D^{*+}, D^0 and D^+ samples, the 30% of D^0 decays, which are also part of the D^{*+} sample, will be included only once in the quoted results.

For each of the three D meson types, the X_E distribution can be described as the sum of three contributions, according to each quark flavour:

$$\frac{1}{N_{Z_h}}\frac{\mathrm{d}N(D\to Kn\pi)}{\mathrm{d}X_E}$$
$$=2B_D[\gamma_{uds}\mathscr{F}_{uds}(X_E)+\gamma_c P_{c\to D}\mathscr{F}_c(X_E,\varepsilon_c)$$
$$+\gamma_b P_{b\to D}\mathscr{F}_b(X_E,\varepsilon_b)], \qquad (2)$$

where N_{Z_h} is the number of collected Z^0 hadronic final states; $N(D)$ is the number of measured D mesons, corrected for acceptance and efficiencies; $\gamma_q=\Gamma_q/\Gamma_h$ ($q=uds,c,b$) stands for the normalised Z^0 partial width ($\gamma_{uds}+\gamma_c+\gamma_b=1$); B_D is the branching fraction $\mathrm{BR}(D\to Kn\pi)$ ($n=1,2$); $P_{c\to D}$ and $P_{b\to D}$ are the probabilities for a c or a b quark to fragment into a D meson, respectively; $\mathscr{F}_q$ is the fragmentation function for each quark flavour.

For light quarks, $\mathscr{F}_{uds}$ describes the probability to generate a D meson after gluon radiation and conversion into a virtual $c\bar{c}$ pair. This contribution is small and is concentrated at low X_E due to the infra-red divergence of the gluon Bremsstrahlung spectrum. In the following, the shape of $\gamma_{uds}\mathscr{F}_{uds}(X_E)$ will be taken from the simulation, where $\langle X_E(D)\rangle_{uds}=0.18$ and with a rate estimated as $5.0\pm2.5\%$ of the charm quark rate $\gamma_c P_{c\to D}$.

For charm and bottom quarks, $\mathscr{F}_{q=c,b}(X_E,\varepsilon_q)$ includes the effects of initial state photon radiation, gluon emission, the Peterson fragmentation [5], and B meson decays for $b\bar{b}$ events. The fragmentation functions $\mathscr{F}_q$ were taken from the simulation. For the bottom quark, the Peterson coefficient ε_b was fixed to 0.008, as quoted in Sect. 2.

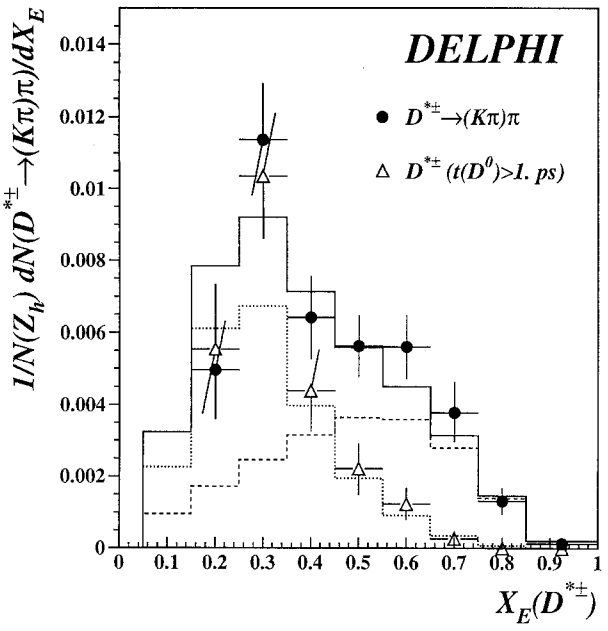

Fig. 6. X_E distributions of all D^{*+} (full dots), and for D^{*+} with a D^0 apparent proper time longer than 1.0 ps (triangles). The data points are corrected for acceptance and reconstruction efficiency. The 9% fraction of $c\bar{c}$ events is subtracted from the triangles. The shape of the Monte Carlo prediction for D^{*+} produced from b quark fragmentation is displayed as a dotted histogram, its normalisation being imposed by a fit to both data samples. The result of the fitted c quark contribution is presented as a dashed histogram. The sum of c and b quark fragmentation contributions is the upper solid line histogram

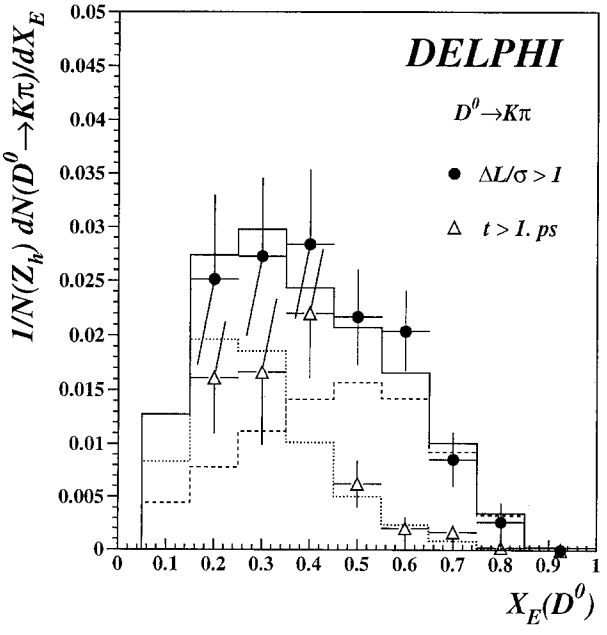

Fig. 7. X_E distributions of D^0 mesons with $\Delta L/\sigma > 1$ (full dots), or apparent proper time above 1 ps (triangles) where the 9% $c\bar{c}$ contribution is subtracted. The histograms are as in Fig. 6

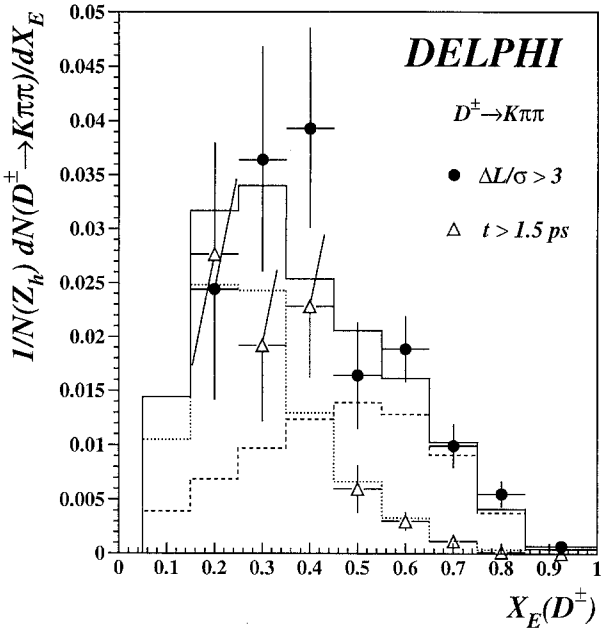

Fig. 8. X_E distributions of D^+ mesons with $\Delta L/\sigma > 3$ (full dots), or apparent proper time above 1.5 ps (triangles) where the 25% $c\bar{c}$ contribution is subtracted. The histograms are as in Fig. 6

For each D meson type, an overall χ^2 fit was performed both to the full sample (with only a $\Delta L/\sigma$ selection for the D^0 and D^+) and to the sample with an apparent proper time selection. The latter is contained in the former, and this was taken into account in the fit. According to equations (1) and (2), the free parameters of the fits were: the fragmentation rates $\gamma_b P_{b\to D} B_D$ and $\gamma_c P_{c\to D} B_D$, and the Peterson parameter ε_c of the charm quark fragmentation function $D_c(z)$.

The X_E distributions are displayed as full dots in Figs. 6, 7 and 8 for the D^{*+}, D^0 and D^+ samples, respectively. The distribution of D^{*+} mesons with a D^0 apparent proper time longer than 1.0 ps is presented as triangles in Fig. 6, where the 9% fraction of $c\bar{c}$ events has been subtracted. This last distribution is found to agree with the $b\to D^{*+}X$ Monte Carlo prediction where the normalisation is obtained from the fit (dotted histograms). It confirms that D mesons from $b\bar{b}$ events have a softer spectrum than D mesons from $c\bar{c}$ events (dashed histograms). A similar behaviour is observed in Figs. 7 and 8 for D^0 and D^+ mesons. The D meson data (full dots) are well fitted by the sum of both $c\bar{c}$ and $b\bar{b}$ contributions (solid line histograms).

Compared to the D^0 and D^+ channels, the D^{*+} distributions have a lower background and a better statistical accuracy. For this reason, the fit to the $X_E(D^{*+})$ distributions is used to determine the Peterson parameter of the charm quark fragmentation function:

$$\varepsilon_c = 0.076\,^{+0.029}_{-0.020}\ (\text{stat}) \pm 0.004\ (\text{sys}) \quad \text{with}$$

$$\Lambda_{\overline{\text{MS}}} = 255\ \text{MeV}, \qquad (3)$$

where the systematic error reflects the uncertainty on the background estimate, the apparent proper time selection

Table 4. D meson production fractions measured in DELPHI (the first error is statistical and the second one is systematic). B_D is the branching ratio BR$(D\to Kn\pi)$ $(n=1, 2)$ of each channel $D^0\to K^-\pi^+$, $D^+\to K^-\pi^+\pi^+$ and $D^{*+}\to D^0\pi^+$ followed by $D^0\to K^-\pi^+$. The Standard Model value $\gamma_b=0.220$ is used for the $P_{b\to D}B_D$ computation. For $P_{b\to D}/P_{c\to D}$, the value $\gamma_c=0.171$ is also assumed

	D^{*+}	D^0	D^+
$\frac{\Gamma(Z^0\to D/\bar{D}X)B_D}{\Gamma_h}$ (%)	$0.425\pm0.029\pm0.026$	$1.47\ \pm0.14\ \pm0.14$	$1.59\ \pm0.15\ \pm0.11$
$\gamma_c P_{c\to D}B_D$(%)	$0.100\pm0.015\pm0.007$	$0.403\pm0.076\pm0.046$	$0.367^{+0.069+0.032}_{-0.075-0.020}$
$P_{b\to D}B_D$(%)	$0.509\pm0.073\pm0.040$	$1.44\ \pm0.27\ \pm0.14$	$1.87\ \pm0.40\ \pm0.21$
$P_{b\to D}/P_{c\to D}$	$0.87^{+0.25}_{-0.20}\pm0.07$	$0.61\ \pm0.20\ \pm0.07$	$0.87\pm0.32^{+0.09}_{-0.14}$

and the ε_b uncertainty, but does not include the choice of the other fragmentation parameters of the simulation. Using $\varepsilon_b=0.008^{+0.005}_{-0.004}$ [6], the ratio $\varepsilon_b/\varepsilon_c$ is found to be $0.11^{+0.08}_{-0.06}$, in agreement with the expectation $(m_c/m_b)^2=0.09\pm0.03$ [5] where the evaluation of the c and b quark masses from [8] is used. From the fitted ε_c value, an average X_E for D^{*+} from charm fragmentation is found to be:

$$\langle X_E(D^*)\rangle_c=0.487\pm0.015\ (\text{stat})\pm0.005\ (\text{sys}), \qquad (4)$$

which is less sensitive to the fragmentation parameters. This result is in agreement with previous analyses at LEP [10][11]. The measured ε_c from D^{*+} was used to describe the shape of the charm quark fragmentation function into D^0 or D^+ mesons.

The D meson production rates are presented in Table 4 together with their statistical and systematic errors. For the first time at LEP, they are measured for charm and bottom quarks separately, and include D^0 and D^+ production. The Z^0 decay rates into D mesons are the sum of *uds*, *c* and *b* quark contributions. The Z^0 and the charm quark decay rates into D^{*+} are in good agreement with the values given in [10] and [11]. Taking the Standard Model values $\gamma_c=0.171$ and $\gamma_b=0.220$, the weighted average of the measured ratio $P_{b\to D}/P_{c\to D}$ is:

$$\left\langle\frac{P_{b\to D}}{P_{c\to D}}\right\rangle=0.76\pm0.15\ (\text{stat})\pm0.06\ (\text{sys}). \qquad (5)$$

It is somewhat lower then the value of 0.96 from the simulation. The difference could be due to a lower fraction, $f_d(b)$, of b quarks fragmenting into $\bar{B}^0$ or B^- (see Sect. 7). The contribution of b-baryon and c-baryon decays into D mesons largely cancel in the ratio. However some channels, which may be underestimated in the simulation, exist only for B meson decays (such as $c\bar{c}$ resonances, D_sK, $\Lambda_c\bar{p}$ or the $b\to uW^-$ transition), and may explain the "charm deficit" which has been observed at the Υ_{4S} [12]. In addition, the D meson selection with X_E above 0.15 could suppress some D^{**} contribution from b quark fragmentation.

The various contributions to the experimental systematic uncertainty are listed in Table 5 for each type of D meson. The systematic error on the reconstruction efficiency was estimated by varying each selection criterion both on the data and on the Monte Carlo samples. It is larger for D^{*+}, due to the D^0 and bachelor pion selections. The uncertainty on the background estimate describes observed differences in the simulation between the fitted number of D mesons and their expected value. In the case of $D^+\to K^-\pi^+\pi^+$, part of the difference is attributed to the reflection of other charmed hadron decays, such as $D_s^+\to K^+K^-\pi^+$ or $\Lambda_c^+\to pK^-\pi^+$. The B lifetime uncertainty affects the data samples where a selection was applied on the normalised decay length or on the apparent proper time. The kaon assignment using $\mathrm{d}E/\mathrm{d}x$ was used for the D^0 and D^+ samples only.

Table 5. Relative systematic uncertainty on the $Z^0\to D/\bar{D}X$ decay rates (experimental contribution)

	D^{*+}	D^0	D^+
Monte Carlo statistics	0.01	0.02	0.02
Background estimate	0.04	0.08	0.06
Reconstruction (without $\mathrm{d}E/\mathrm{d}x$)	0.04	0.03	0.03
$\mathrm{d}E/\mathrm{d}x$ selection	–	0.03	0.02
B lifetime ($\tau(B)=1.3\pm0.1$ ps)	–	0.01	0.01
$\varepsilon_b\left(=0.008^{+0.005}_{-0.004}\right)$	0.01	0.01	0.01
Light flavours	0.01	0.01	0.01
Total	0.06	0.09	0.07

Using the D meson branching fractions $B_0=$ BR$(D^0\to K^-\pi^+)=0.0365\pm0.0021$, $B_+=$ BR$(D^+\to K^-\pi^+\pi^+)=0.080\pm0.008$ [8] and $B^*=$ BR$(D^{*+}\to D^0\pi^+)=0.681\pm0.016$ [13], the fractional decay widths of the Z^0 into D mesons are measured:

$$\begin{aligned}&\Gamma(Z^0\to D^{*\pm}X)/\Gamma_h\\&=0.171\pm0.012\ (\text{stat})\\&\quad\pm0.011\ (\text{sys. exp})\pm0.011\ (\text{sys. BR}),\\&\Gamma(Z^0\to D^0/\bar{D}^0X)/\Gamma_h\\&=0.403\pm0.038\ (\text{stat})\\&\quad\pm0.038\ (\text{sys. exp})\pm0.023\ (\text{sys. BR}),\end{aligned} \qquad (6)$$

Table 6. D meson production rates measured at the Υ_{4S} (the first error is statistical, the second is systematic and includes, in the case of charm fragmentation, a 8.5% relative contribution which is common to each D meson)

	D^{*+}	D^0	D^+
$P_{c\to D} B_D$(%) [14]	$0.690 \pm 0.061 \pm 0.081$	$2.11 \pm 0.20 \pm 0.20$	$2.07 \pm 0.28 \pm 0.19$
BR$(B\to \bar{D}X) B_D$(%) [15]	$0.630 \pm 0.030 \pm 0.062$	$2.18 \pm 0.09 \pm 0.13$	$2.17 \pm 0.20 \pm 0.17$

$$\Gamma(Z^0\to D^{\pm} X)/\Gamma_h$$
$$= 0.199 \pm 0.019 \text{ (stat)}$$
$$\pm 0.014 \text{ (sys. exp)} \pm 0.020 \text{ (sys. BR)},$$

where the branching ratios into ground state D mesons include the contributions from D^*.

Similar analyses of D meson production have been published on the *same* decay channels at centre-of-mass energies around the Υ_{4S}: below the $B\bar{B}$ threshold for the charm quark fragmentation [14], and at the Υ_{4S} for the B meson branching fractions [15]. They are summarized in Table 6, where CLEO and ARGUS branching ratios for B mesons are combined. In the following, the DELPHI and Υ_{4S} measurements will be compared.

5 Discussion on primary D mesons

In this section, the nature of the primary D meson will be discussed. In charm quark fragmentation or in B meson decay, the *primary* D can be a D^{**}, a D^* or a D meson. Subsequently the D^{**} decays into D^* or into D. Whereas D^* branching fractions are now accurately measured [13], very little is known about D^{**} production and decay [16].

The difference between the D^0 and D^+ production fractions arises from the observed $(D^{*+}\to D^0\pi^+)$ fraction, Y, while D^{*0} always decay to D^0. If $f_d(c)$ is defined as the probability for a charm quark to fragment into a primary charged D, D^* or D^{**} meson (assumed equal to $f_u(c)$, similarly defined for the fragmentation to a neutral D meson), then the probabilities for a charm quark to fragment into *final* state D mesons are expressed as:

$$\begin{aligned} P_{c\to D^{*+}} B_* &= Y f_d(c), \\ P_{c\to D^0} &= (1+Y) f_d(c), \\ P_{c\to D^+} &= (1-Y) f_d(c). \end{aligned} \tag{7}$$

In the absence of D^{**} production, $Y = B_* P_V$ where $P_V = V/(V+P)$ is defined as the ratio of the primary vector meson rate to the total primary vector + pseudoscalar meson rate, and B_* as the branching fraction BR$(D^{*+}\to D^0\pi^+)$.

In fact the fraction of D^{*+} mesons produced depends also on the probability, H, for a charm quark to fragment into a D^{**+} and on the average branching fraction $B_{**} = \text{BR}(D^{**}\to D^{*+}X)$ (assumed to be identical to $D^{*0}X$ decay). Then the above set of equations (7) remains valid if the observed D^{*+} rate is defined as:

$$Y = B_*[H(2B_{**} - P_V) + P_V], \tag{8}$$

where the same notation as in [11] is used. Therefore from the measurement of Y, information on D^{**} as well as on P_V may be obtained.

The same relations (7-8) hold for b quark fragmentation where $f_d(c)$ is replaced by $f_d(b)$, the probability for a b quark to fragment into a charged or neutral B meson (assumed to be identical). However $\bar{B}_s$ meson and b-baryons, produced with a b fragmentation probability $f_s + f_{\Lambda_b} \equiv 1 - 2f_d(b)$, may decay into final state D mesons. The average branching ratio of $\bar{B}_s$ and b-baryons decaying to D mesons is assumed to be a fraction b_s of the B meson branching ratio BR$(B\to\bar{D}X)$. Then $f_d(c)$ in (7) has to be replaced by BR$(B\to\bar{D}X)$ $[2f_d(b) + b_s(1-2f_d(b))]$.

As a cross-check on this formulation, when adding $c\bar{c}$ and $b\bar{b}$ contributions, the following ratio is found compatible with the expected value of 1:

$$\frac{\Gamma(Z^0\to D^0/\bar{D}^0 X) - \Gamma(Z^0\to D^{\pm} X)}{2\Gamma(Z^0\to D^{*\pm} X) B_*}$$
$$= 0.88 \pm 0.19 \text{ (stat)} \pm 0.17 \text{ (sys.exp)}$$
$$\pm 0.10 \text{ (sys. BR)}, \tag{9}$$

where the last systematic error includes the error on the D^0 and D^+ branching ratios [8]. The observed fraction of D^{*+} produced, Y, has been obtained from a χ^2 fit to (7), for $c\bar{c}$ and $b\bar{b}$ events separately:

$$\begin{aligned} Y(c) &= 0.367 \pm 0.056 \text{ (stat)} \\ &\quad \pm 0.021 \text{ (sys. exp)} \pm 0.027 \text{ (sys. BR)}, \\ Y(b) &= 0.377 \pm 0.060 \text{ (stat)} \\ &\quad \pm 0.031 \text{ (sys. exp)} \pm 0.027 \text{ (sys. BR)}. \end{aligned} \tag{10}$$

These values are close to those measured around the Υ_{4S}: $Y(c) = 0.426 \pm 0.039$ (stat) ± 0.030 (sys. exp) ± 0.028 (sys. BR) and $Y(b) = 0.394 \pm 0.023$ (stat) ± 0.030 (sys. exp) ± 0.027 (sys. BR); see Table 6.

In the absence of D^{**} production and if P_V is equal to 0.75, the naive spin counting expectation, a value of $Y \equiv B_* P_V = 0.51 \pm 0.01$ is expected. The value of Y would be reduced to 0.34 ± 0.01 if a value of $P_V = 0.5$ was used. Both the Υ_{4S} and DELPHI data favour a D^{*+} fraction corresponding to P_V lower than 0.75 if there is no D^{**} production.

However D^{**} mesons have been observed [16]. The measured value of Y is compatible with $P_V = 0.75$ if the branching fraction $B_{**} = \text{BR}(D^{**}\to D^{*+}X)$ is lower than $P_V/2 = 0.38$, according to (8). This ambiguity will be resolved with more accurate data and direct D^{**} measurements.

6 Measurement of the Z^0 partial width Γ_c/Γ_h

The Z^0 partial width into charm quark pairs can be inferred from the DELPHI and CLEO [14] measurements. In $c\bar{c}$ events from Z^0 decays, the fraction of D mesons produced is proportional to Γ_c/Γ_h times the probability for a charm quark to fragment into a final state D meson, whereas only this probability is involved at centre-of-mass energies around 10 GeV. Two measurements of Γ_c/Γ_h will be presented, the second one relying on less arbitrary assumptions.

If the D^{**}, D_s and charm-baryon production ratios are assumed to be similar at LEP energies and at around 10 GeV, then combining the D^{*+}, D^0 and D^+ decay channels leads to:

$$\frac{\Gamma_c}{\Gamma_h} = \frac{(\gamma_c P_{c\to D} B_D)_{\text{DELPHI}}}{(P_{c\to D} B_D)_{\text{CLEO}}}$$
$$= 0.161 \pm 0.020\ (\text{stat}) \pm 0.019\ (\text{sys}), \qquad (11)$$

where the systematic uncertainty is dominated by the 8.5% normalisation uncertainty of CLEO.

Since all D^{**} decay into D^* or D mesons (neglecting D^{**} decay into $D_s K$), then Γ_c/Γ_h can be measured assuming only that the production of D_s and charm-baryons by primary charm quarks is equal at LEP energies and at around 10 GeV:

$$\frac{\Gamma_c}{\Gamma_h} = \frac{(\gamma_c P_{c\to D^0} + \gamma_c P_{c\to D^+})_{\text{DELPHI}}}{(P_{c\to D^0} + P_{c\to D^+})_{\text{CLEO}}}$$
$$= 0.187 \pm 0.031\ (\text{stat}) \pm 0.023\ (\text{sys}). \qquad (12)$$

If the fraction of D_s (or charm-baryons) was to differ by 10% at LEP energies and at around 10 GeV, the value of Γ_c/Γ_h would change by about 0.002 in (12). Half of the systematic uncertainty is due to the CLEO normalisation. The errors on the D^0 and D^+ branching fractions now contribute to the systematic error, although they partially cancel in the ratio. These measurements are in good agreement with the Standard Model expectation $\gamma_c = 0.171$.

7 Measurement of $f_d(b)$

Using similar arguments to those above, the probability $f_d(b)$ for a b quark to fragment into $\bar{B}^0$ (or B^-) meson in Z^0 hadronic decays can be inferred from DELPHI and Υ_{4S} [15] measurements. In the latter case, $\bar{B}_s$ or b-baryon production is kinematically forbidden, and $f_d(b)$ is 0.5 at the Υ_{4S}. Hence the probability for a b quark to fragment into a D meson at LEP energies can be expressed as:

$$P_{b\to D} B_D = \text{BR}(B\to \bar{D}X)\, B_D [2 f_d(b) + b_s(1 - 2 f_d(b))], \qquad (13)$$

where B_D is the branching ratio $\text{BR}(D\to Kn\pi)$ ($n = 1, 2$) and the fraction b_s, defined in Sect. 5, is assumed to be 0.1 ± 0.1. The branching fractions $\text{BR}(B\to \bar{D}X)\, B_D$ are listed in Table 6 from Υ_{4S} data. The rates $P_{b\to D} B_D$ are measured in DELPHI and listed in Table 4, assuming the Standard Model value $\gamma_b = 0.220$. Then $f_d(b)$ can be measured for each D meson and a weighted average value computed:

$$f_d(b) = \frac{1}{2(1-b_s)} \times \left[\frac{(P_{b\to D} B_D)_{\text{DELPHI}}}{\text{BR}(B\to \bar{D}X)\, B_D)_{\Upsilon_{4S}}} - b_s \right]$$
$$= 0.366 \pm 0.047\ (\text{stat}) \pm 0.048\ (\text{sys. exp}) \pm 0.015\ (\text{sys. } b_s) \qquad (14)$$

in agreement with the value $f_d(b) = 0.40$ of the simulation. Both DELPHI and Υ_{4S} results contribute a similar systematic uncertainty. The probability for a b quark to fragment into $\bar{B}_s$ or b-baryon is inferred:

$$f_s + f_{\Lambda_b} \equiv 1 - 2 f_d(b)$$
$$= 0.268 \pm 0.094\ (\text{stat}) \pm 0.096\ (\text{sys. exp}) \pm 0.030\ (\text{sys. } b_s). \qquad (15)$$

This measurement confirms and improves a recent one based only on $B\to \bar{D}\ell^+ X$ decays [17].

8 Conclusion

From 263 700 Z^0 hadronic decays collected in 1991, charmed mesons were reconstructed using the channels $D^0\to K^-\pi^+$, $D^+\to K^-\pi^+\pi^+$ and $D^{*+}\to D^0\pi^+$ followed $D^0\to K^-\pi^+$. The D meson apparent proper time was used to select an enriched sample of B decay events. From the observed $X_E(D) = E(D)/E_{\text{beam}}$ distributions, the production fraction of each D meson in Z^0 hadronic decays is measured for the first time for $c\bar{c}$ and for $b\bar{b}$ events separately. The relative probabilities for b and c quarks to fragment into a final state D meson is found to be in average:

$$\left\langle \frac{P_{b\to D}}{P_{c\to D}} \right\rangle = 0.76 \pm 0.15\ (\text{stat}) \pm 0.06\ (\text{sys}).$$

The average energy fraction of D^{*+} in charm quark fragmentation function is obtained:

$$\langle X_E(D^*)\rangle_c = 0.487 \pm 0.015\ (\text{stat}) \pm 0.005\ (\text{sys}),$$

and the fractional decay widths of the Z^0 into D mesons are measured to be:

$$\Gamma(Z^0\to D^{*\pm}X)/\Gamma_h = 0.171 \pm 0.012\ (\text{stat}) \pm 0.016\ (\text{sys}),$$
$$\Gamma(Z^0\to D^0/\bar{D}^0 X)/\Gamma_h = 0.403 \pm 0.038\ (\text{stat}) \pm 0.044\ (\text{sys}),$$

$$\Gamma(Z^0 \to D^{\pm} X)/\Gamma_h$$
$$= 0.199 \pm 0.019\ (\text{stat}) \pm 0.024\ (\text{sys}),$$

where the branching ratios into ground state D mesons include the contributions from D^*.

Comparing these results for $c\bar{c}$ and $b\bar{b}$ events separately with those measured around the Υ_{4S} [14, 15], some D^{**} production would be favoured with a branching fraction BR$(D^{**} \to D^{*+} X)$ lower than 0.38 if the ratio P_V of primary vector mesons to vector + pseudoscalar mesons equals 0.75. Otherwise a lower value for P_V would be favoured.

Assuming that the fraction of primary charm quarks fragmenting to D_s and charm-baryons is equal at LEP energies and at around 10 GeV, the Z^0 partial width into charm quark pairs is determined:

$$\frac{\Gamma_c}{\Gamma_h} = 0.187 \pm 0.031\ (\text{stat}) \pm 0.023\ (\text{sys}).$$

Assuming the Standard Model value $\Gamma_b/\Gamma_h = 0.220$, the probability $f_d(b)$ for a b quark to fragment into $\bar{B}^0$ (or B^-) is measured to be:

$$f_d(b) = 0.366 \pm 0.047\ (\text{stat}) \pm 0.050\ (\text{sys})$$

and the probability for a b quark to fragment into $\bar{B}_s$ or b-baryon is inferred:

$$f_s + f_{\Lambda_b} \equiv 1 - 2 f_d(b)$$
$$= 0.268 \pm 0.094\ (\text{stat}) \pm 0.100\ (\text{sys}).$$

Acknowledgements. We are greatly indebted to our technical collaborators and to the funding agencies for their support in building and operating the DELPHI detector, and to the members of the CERN-SL Division for the excellent performance of the LEP collider.

References

1. P. Aarnio et al., DELPHI Coll.: Nucl. Instrum Methods A303 (1991) 233
2. N. Bingefors et al.: CERN-PPE/92-173 (1992), Nucl. Instrum. Methods, to be published
3. T. Sjöstrand: Comput. Phys. Commun. 39 (1986) 347; T. Sjöstrand, M. Bengtsson: Comput. Phys. Commun. 43 (1987) 367; T. Sjöstrand: JETSET 7.3 manual, preprint CERN-TH 6488/92 (1992)
4. T. Todorov: Thèse, Université Louis Pasteur, CRN Strasbourg (1993), (unpublished)
5. C. Peterson et al.: Phys. Rev. D27 (1983) 105
6. P. Abreu et al., DELPHI Coll.: Z. Phys. C56 (1992) 47
7. DELSIM Reference Manual, DELPHI 87-98 PROG 100, Geneva, 1989
8. Review of Particle Properties (Particle Data Group): Phys. Rev. D45 (1992) vol. 11-II
9. P. Abreu et al., DELPHI Coll.: Z. Phys. C53 (1992) 567
10. G. Alexander et al., OPAL Coll.: Phys. Lett. B262 (1991) 341
11. D. Decamp et al., ALEPH Coll.: Phys. Lett. B266 (1991) 218
12. M.V. Danilov: Heavy Flavour Physics, in: Proc. Joint International Lepton-Photon & Europhysics Conference on High Energy Physics, Geneva, Switzerland, 1991, Vol. 2, p. 341, S. Hegarty, K. Potter, E. Quercigh (eds.). Singapore: World Scientific 1992
13. F. Butler et al.: CLEO Coll.: Phys. Rev. Lett. 69 (1992) 2041
14. D. Bortoletto et al., CLEO Coll.: Phys. Rev. D37 (1988) 1719; Phys. Rev. D39 (1989) 1471
15. H. Albrecht et al., ARGUS Coll.: Z. Phys. C52 (1991) 353; D. Bortoletto et al., CLEO Coll.: Phys. Rev. D45 (1992) 21
16. H. Albrecht et al., ARGUS Coll.: Phys. Rev. Lett. 56 (1986) 549; Phys. Lett. B221 (1989) 422; Phys. Lett. B230 (1989) 162; Phys. Lett. B232 (1989) 398; Phys. Lett. B297 (1992) 425; Z. Phys. C57 (1993) 533; J.C. Anjos et al., E691 Coll.: Phys. Rev. Lett. 62 (1989) 1717; P. Avery et al., CLEO Coll.: Phys. Rev. D41 (1990) 774
17. P. Abreu et al., DELPHI Coll.: Z. Phys. C57 (1993) 181